

# Effects of the Operating Parameters on the Reverse Osmosis-Electrodeionization Performance in the Production of High Purity Water

Jung-Hoon Song, Kyeong-Ho Yeon, Jaeweon Cho and Seung-Hyeon Moon<sup>†</sup>

Department of Environmental Science and Engineering, Gwangju Institute of Science and Technology (GIST),  
1 Oryong dong, Buk-gu, Gwangju 500-712, South Korea  
(Received 30 June 2004 • accepted 26 October 2004)

**Abstract**—An RO-CEDI (Reverse osmosis-continuous electrodeionization) hybrid process was investigated to produce high purity water. The RO system, with an effective membrane area of 1.1 m<sup>2</sup>, was operated using tap water with conductivity of 64  $\mu\text{s}\cdot\text{cm}^{-1}$ , and the CEDI system experiments were carried out in a cell-pair stack consisting of 3 compartments. During the parametric study of the RO-CEDI hybrid system, the optimal operating conditions were determined based on the water purity. The electrical resistivity and water dissociation of the ion exchange resins and ion exchange membrane were verified as the key mechanisms of the CEDI system in the water purification. The produced water met the quality requirements as a make-up water in a nuclear power plant with a resistivity of 10-16.7 M $\Omega\cdot\text{cm}$ .

Key words: Continuous Electrodeionization, RO-CEDI Hybrid Process, Make-up Water, High Purity Water

## INTRODUCTION

The RO-IX (Reverse osmosis-Ion exchange) process is now broadly used as the final water treatment step to produce high purity water in a nuclear power plant due to its high decontamination efficiency, simplicity, and easy operation [Noh et al., 1996; Spiegler, 1966]. However, the generally used IX (Ion exchange) process not only requires regular chemical-regeneration but also produces secondary wastewater, composed of both a strong acid and strong base. These problems have recently become more significant as environmental concerns on salt waste have increased [Yeon, 2003a].

The continuous electrodeionization (CEDI) process is a novel hybrid separation process, consisting of electrodialysis and ion exchange. Application of CEDI systems is now expanding because the system enables regeneration of the resin continuously without chemical use. As a result, it is considered as an environmentally friendly process, and it has taken center stage as a possible alternative process for IX in production of high purity water [Yeon et al., 2004b; Walters et al., 1955; Ganzi et al., 1987, 1992; Spiegel et al., 1999; Thate et al., 1999].

It is known that the CEDI process produces high purity water at a resistivity of over 15 M $\Omega\cdot\text{cm}$  and its removal mechanism for ionic species is typically explained by the theory of two distinct operating regimes [Yeon, 2003a]. However, the effects of operating parameters and removal mechanisms were not elucidated due to electrochemical complexity of the CEDI system. Thus, the purpose of this study is to investigate the effects of the operating parameters on the CEDI system and to apply these results to produce high purity water. Prior to the investigation of the CEDI system, the RO system was optimized in terms of operating conditions. The mechanism of the CEDI system was also studied to prove the two distinctive regimes in the ion exchange resin. The quality of the water produced using the RO-CEDI was evaluated according to the water quality require-

ments for the nuclear power plant.

## EXPERIMENTAL

### 1. Materials

Tap water with conductivity of 64  $\mu\text{s}\cdot\text{cm}^{-1}$  was used as the RO feed solution and the RO permeate was used as the CEDI feed solution. The feed solution adjusted with 1 N NaCl in the tap water was used for investigation of the effect of the feed conductivity in the RO and CEDI systems. A polyamide type of CSM membrane (Saehan Co. Ltd, South Korea) was used in an RO module with effective membrane area of 1.1 m<sup>2</sup>. The CEDI system with an effective membrane area of 5 $\times$ 10 cm<sup>2</sup> was employed in this study. The dilute compartment had a thickness of 10 mm. Amberlite nuclear grade IRN77 and IRN78 (Rohm & Haas Co., USA) were packed into the dilution gasket, while CMX and AMX membranes (Tokuyama Soda Co. Ltd., Japan) were used for the compartment. The schematic process diagram is shown in Fig. 1.

### 2. Characterization of Diluate Compartment

The void fraction of the IRN77 and IRN78 resins was measured to calculate the velocity of the interstitial solution in the CEDI system. Swollen resin was used in the dilution gasket of the CEDI system, which had dimensions of 5 cm $\times$ 10 cm $\times$ 1 cm, and then the

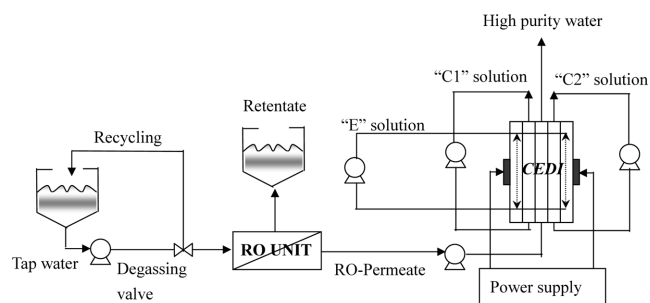


Fig. 1. Process diagram for RO-CEDI hybrid system (C1: cathodic concentrate, C2: anodic concentrate, E: Electrode rinse).

<sup>†</sup>To whom correspondence should be addressed.  
E-mail: shmoon@gist.ac.kr

**Table 1. Operating conditions in RO system**

Experiment	Operating conditions	Temperature (°C)	Pressure (Kg·cm <sup>-2</sup> )	Feed conductivity (μs·cm <sup>-1</sup> )	Recovery rate (%)	Feed pH	Feed TOC (ppm)
Temperature	Varied	10	64	15	6.4	2.33	
Pressure	15	Varied	64	15	6.4	2.33	
Conductivity	15	10	Varied	15	6.4	NM*	
Recovery	15	10	64	Varied	6.4	NM*	

NM\*: Not measured.

**Table 2. Operating conditions in CEDI system**

Experiment	Operating conditions	Temperature (°C)	Flow rate (ml·min <sup>-1</sup> )	Current density (A·m <sup>-2</sup> )	Feed conductivity (μs·cm <sup>-1</sup> )	Feed TOC (ppm)
Temperature	Varied	10	20 (40 V*)	2.3	0.108	
Flow rate	25	Varied	20	2.3	0.108	
Current density	25	10	Varied	2.3	0.108	
Feed conductivity	25	10	20	Varied	NM*	

NM\*: Not measured.

40 V\*: CEDI was also carried out with constant voltage mode under 40 volt.

weight of the ion exchange resin was measured. Ten samples of the ion exchange resin from the dilute compartment were selected, and the diameter and weight of each sample were measured to calculate the average density of the ion exchange resin. The void fraction of the ion exchange resin in the CEDI system was calculated by the following equation.

$$\varepsilon(\text{void fraction}) = \frac{V_i - V_s}{V_i} = \frac{V_i - \frac{W_m}{\rho}}{V_i} \quad (1)$$

where,  $V_i$  : total volume in the diluted compartment

$V_s$  : total volume taken by the ion exchange resin in diluted compartment

$W_m$  : weight of the ion exchange resin in the diluted compartment

$\rho$  : density of the ion exchange resin in the diluted compartment

A flow cell was used to measure the electrical conductivity of the saturated media. Saturated media was prepared with sodium hydroxide and hydrochloric acid (sodium hydroxide was used for preparation the of Na<sup>+</sup> and OH<sup>-</sup> forms of the resin and hydrochloric acid for preparation of the H<sup>+</sup> and Cl<sup>-</sup> forms). The electrical conductivity of the resin beds was measured with an LCZ meter with the flow cell at 1.5 cm·sec<sup>-1</sup> [Helfferich, 1962; Yeon et al., 2003b]. The cell constant was calculated by using a solution having a known k value, while the LCZ meter provided the resistance, R. Therefore, k can be determined from Eq. (2).

$$R = \frac{l}{kA} \quad (2)$$

where,  $l$ =distance between the electrodes,  $A$ =area of the electrode

### 3. RO-CEDI Operation

The RO-CEDI system was operated under various operating parameters. For each experiment, only one parameter among these

was varied, as shown in Tables 1 and 2. The produced RO permeate under the optimal conditions was used as the feed solution for the CEDI system. The CEDI system was then operated to investigate the effects of various operating parameters on the production of high purity water. Experiments with the CEDI system were carried out with 1 cell pair having 3 compartments. The dilute compartment has a thickness of 10 mm and the cell configuration is shown in Fig. 2. The experiments were conducted with a mixed bed in the dilute compartment. Pt electrodes were inserted in the dilute compartment to examine the CEDI mechanism in this stack configuration. Regenerated nuclear grade cation/anion exchange resins with sodium and chloride form, respectively, were mixed to make 2 to 3 volume ratio [Yeon et al., 2004]. Na<sub>2</sub>SO<sub>4</sub> solution of 500 μs·cm<sup>-1</sup> was used as initial electrolyte rinse solution in the concentrate compartment "C" and in electrode compartment "E" as shown in Fig. 2.

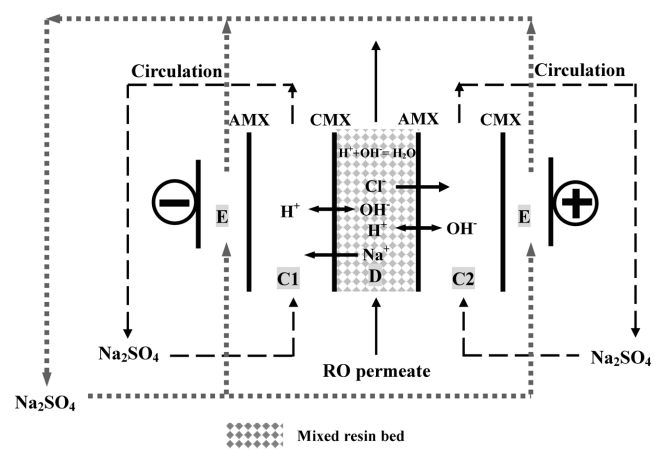


**Fig. 2. Mixed bed configuration in the diluate compartment (CMX: cation exchange membrane, AMX: anion exchange membrane, C1: cathodic concentrate, C2: anodic concentrate, D: diluate, E: electrode rinsing).**

RO permeate and CEDI effluent were analyzed by ion chromatography (DX-500, DIONEX, U.S.A.), TOC meter (Sievers 820, Sievers Instrument Inc., USA), and ICP-AES (Thermo Jarrell Ash IRIS/AP). A conductivity meter (Cole-Parmer) and pH meter (Orion) were used to measure conductivity and pH during the RO-CEDI operation.

## RESULTS AND DISCUSSION

### 1. Determination of Optimal Feed Conditions for CEDI using

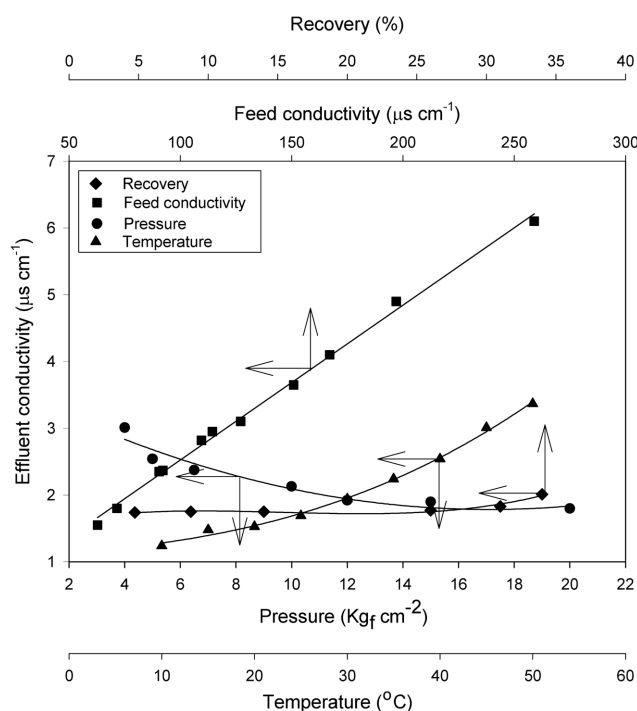


Fig. 3. Effect of operating variables on conductivity of RO permeate.

Table 3. Raw water and CEDI effluent quality

Parameter	CEDI feed (RO permeate)	CEDI effluent
pH	6.4	7.4
TOC (ppm)	0.108	0.088
Conductivity ( $\mu\text{s}\cdot\text{cm}^{-1}$ )	2.3	0.06 (16.7 $\text{M}\Omega\cdot\text{cm}$ )
Dissolved $\text{SiO}_2$ (ppm)	1.03	<0.02
Cations (ppb)		
$\text{Ca}^{2+}$	250	4
$\text{Mg}^{2+}$	63	2
$\text{Na}^+$	35	ND*
Anions (ppb)		
$\text{Cl}^-$	12	4
$\text{NO}_3^-$	13	ND*
$\text{SO}_4^{2-}$	7	ND*

a)ND\*: Not detected.

b)Detection limit for ion chromatography (DX-500, DIONEX): 1 ppb.

January, 2005

### RO Membrane

RO membrane was used for removal of organic matters and ionic species as a pretreatment system to produce high purity water. Conductivity was measured to determine the optimal operating conditions in the RO system for pretreatment. Fig. 3 shows the conductivity of the RO permeate with feed conductivities, pressures, recovery rates, and pressures. Changes in the conductivity in the range of general operating conditions for the RO system were still lower than  $6.5 \mu\text{s}\cdot\text{cm}^{-1}$ . Based on the above results, the optimal operating conditions are determined to be  $15^\circ\text{C}$ ,  $10 \text{ kg}\cdot\text{cm}^{-2}$ , and  $64 \mu\text{s}\cdot\text{cm}^{-1}$  for the temperature, pressure, and feed conductivity, respectively. Table 3 shows the qualities of RO permeate under the optimal operating conditions. Under the conditions, the permeate water quality was observed to be  $2.3 \mu\text{s}\cdot\text{cm}^{-1}$  and the effluent TDS was determined to be 0.108 ppm, which implies that the RO system was effective in the removal of organic matter.

### 2. Production of High Purity Water using a CEDI System After RO

The removal efficiency of the CEDI system is usually expressed by the effluent conductivity or resistivity, and salt removal (%). Therefore, this study focused on the removal rates and resistivities.

#### 2-1. Effect of Temperature

In this experiment, the RO permeate ( $2.3 \mu\text{s}\cdot\text{cm}^{-1}$ ) was used as a feed solution and CEDI stack was operated with the flow rate of  $10 \text{ ml}\cdot\text{min}^{-1}$  either under a constant current mode at  $20 \text{ A}\cdot\text{m}^{-2}$  or under a constant voltage mode at 40 volts as shown in Table 2. Fig. 4 shows the resistivity and removal rate of the effluent solution when the feed temperature was varied in the range of  $10^\circ\text{C}$  to  $35^\circ\text{C}$ . From the result of the constant current operation, the removal rate and effluent conductivity did not change regardless of the temperature variation. However, a different result was observed during the constant voltage operation. In a constant voltage mode, the effluent resistivity increased as the temperature was increased. Moreover, a  $16.7 \text{ M}\Omega\cdot\text{cm}$  permeate solution was obtained when the temperature was greater than  $25^\circ\text{C}$ , because the higher temperature increased ionic mobility in the solution. If the mobility is large enough, the ions move more easily to the membranes through the ion exchange resins

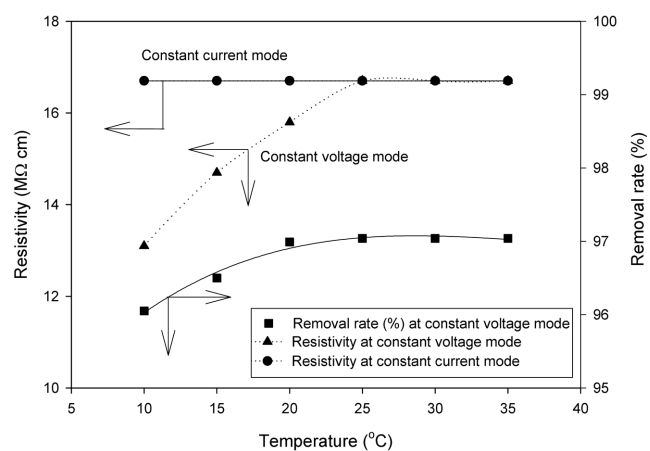


Fig. 4. Effect of the temperature on the effluent resistivity and removal rate (Constant current mode: operation at current density  $20 \text{ A}\cdot\text{m}^{-2}$ , Constant voltage mode: operation at stack voltage 40 Volts, Flow rate:  $10 \text{ ml}\cdot\text{min}^{-1}$ ).

under the same electrical potential. Moreover, this effect decreased the stack resistance and, as a result, more current flowed through the stack according to Ohm's law, which also enhanced the removal rate in the effluent solution.

### 2-2. Effect of Flow Rate

Effects of the flow rate were investigated with various feed flow rates in the range of 2 to 40 ml·min<sup>-1</sup>. To express the mean interstitial velocity of the fluid, the void fraction was calculated. The densities of IRN 77 and IRN 78 were found to be 1.27 g·ml<sup>-1</sup> and 1.22 g·ml<sup>-1</sup>, respectively. Using Eq. (1) with the weight of resins packed in the dilution gasket, the void fraction ( $\epsilon$ ) was calculated as 0.342 for IRN77, and 0.434 for IRN78, the average void fraction ( $\epsilon_{avg}$ ) being 0.392. The mean interstitial velocity of the fluid was then calculated by the following Eq. (4):

$$U_e = \frac{Q}{\epsilon_{avg} A} = \frac{U}{\epsilon_{avg}} \quad (4)$$

where, Q : volume flow rate

A : cross-sectional area of the dilute compartment

$\epsilon_{avg}$  : average void fraction (0.392)

U : superficial speed of the fluid

Fig. 5 shows the changes in the resistivity and removal rate of the effluent solution according to the interstitial velocity of the fluid in CEDI stack. The rejection rate was found to be inversely proportional to the feed flow rate. From Fig. 5, the effluent resistivity was 16.7 M $\Omega$ ·cm when the interstitial velocity of the fluid was lower than 10 cm·min<sup>-1</sup>. However, the resistivity decreased rapidly when the solution flow rate was greater than this and appeared to be caused by a decreased contact time with the ion exchange resins in the CEDI stack, under which condition sorption equilibrium was not attained. A decrease in the sorption further lowered the electromigration rate to ion exchange membrane, leading to a decrease in the removal rate and the effluent resistivity.

### 2-3. Effects of the Feed Conductivity

The effects of the feed conductivity are shown in Fig. 6. The feed conductivity was varied from 2.3  $\mu$ S·cm<sup>-1</sup> to 30  $\mu$ S·cm<sup>-1</sup> by mixing the feed water with a NaCl solution and the effluent resistivity was measured. As shown in Fig. 6, the feed conductivity was inversely

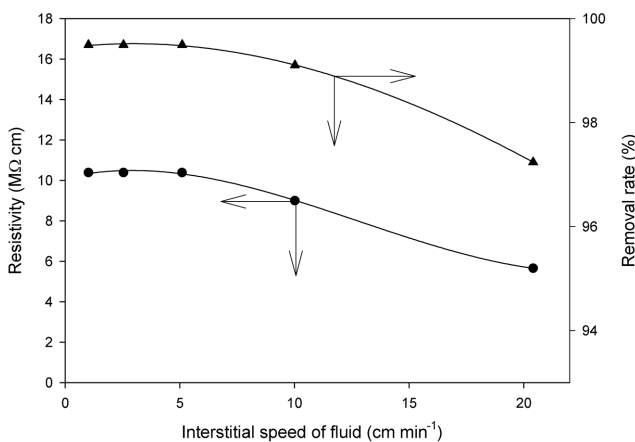


Fig. 5. Effect of the interstitial speed of fluid on the effluent resistivity and removal rate (Current density 20 A·m<sup>-2</sup>, Feed temperature: 25 °C, Feed conductivity: 2.3  $\mu$ S·cm<sup>-1</sup>).

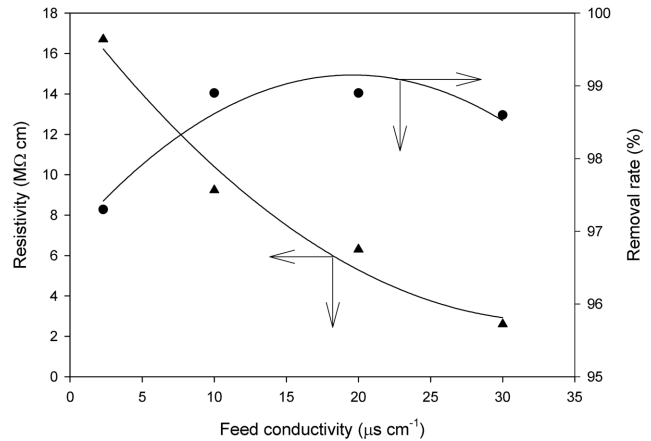


Fig. 6. Effect of the feed conductivity on the effluent resistivity and removal rate.

proportional to the effluent resistivity, giving the steep changes in the resistivity of produced water. The steep changes in the produced resistivity may be caused by the changing exchange zone of the CEDI system. It is usually accepted that ion exchange resins have high preferences under a low concentration of feed solution [Helfferich, 1962]. The high preference induces a sharp exchange zone boundary in the CEDI system with high efficiency. On the other hand, the exchange zone boundary of the CEDI system becomes dispersed at a high feed concentration. The dispersed exchange zone induces easy breakthrough of ions and then degrades water quality. Thus, a high feed concentration directly leads to the steep degradation of performance of a CEDI system. Thus, it is reasonable that the conductivity of feed water is also an important criterion for the produced water quality and efficiency of a CEDI system. Also, the feed solution of CEDI must be controlled in a pretreatment system such as RO.

### 2-4. Effects of the Current Density

The effect of the current density is shown in Fig. 7. The effluent resistivity was 16.7 M $\Omega$ ·cm when the current density was greater than 20 A·m<sup>-2</sup>. Neither the resistivity nor the removal rate increased further when the current density was higher than 20 A·m<sup>-2</sup>, indicat-

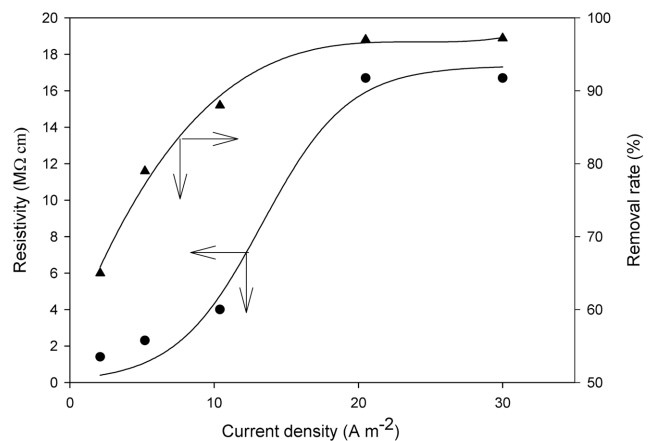


Fig. 7. Effect of the current density on the effluent resistivity and removal rate.

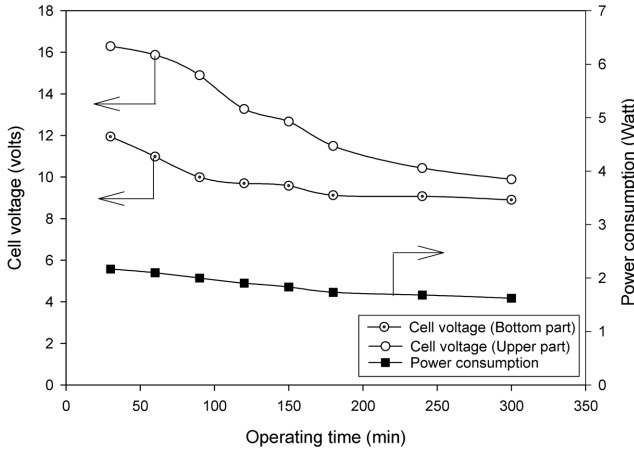


Fig. 8. Cell voltage, power consumption, energy consumption according to time.

ing that all the ions were removed at the current density. The current density was considered as optimal for the feed solution. Ionic depletions in the electroregeneration region resulted in the development of high voltage gradients. Under the conditions, the voltage gradient on the resin surfaces exceeded the thermodynamic potential of 0.83 volts and the high potential caused catalytic reactions for water splitting, or decomposition to form hydrogen and hydroxide ions, which may be used for regeneration of ion exchange resins.

### 3. Performance of the CEDI System

#### 3-1. Transport Mechanism in a CEDI System

Typical CEDI systems have two distinctive regions, referred to as the enhanced transfer region located in the bottom area and electroregeneration region located in upper area [Yeon, 2003a]. To verify this mechanism, Pt electrodes were inserted in the upper and lower regions of the cell and the voltage difference between the upper and lower areas in the CEDI stack was measured. Fig. 8 shows the voltage change between the upper and lower parts in the CEDI system. It was found that the lower regions have a lower resistance than the upper regions, and the resistances in both areas decreased with the elapsed time.

The difference of the two regions in Fig. 8 indicates that there exist two distinct operating regimes with height, namely “enhanced transfer” and “electroregeneration.” In the “enhanced transfer” regime, both an ion-exchange and electro-migration occurs. This causes most ions to be depleted and then cell resistance increased as the stack height increased. In the “electroregeneration” regime in the upper part, an increase in the resistance with the height results in a potential increase under a constant current operation. Then, water splitting occurs and ion exchange resin is continuously regenerated. Thus, the enhanced transfer region has a lower voltage drop due to lower resistance than the electroregeneration region under constant current mode operation. This can explain the voltage changes of upper and bottom parts in the CEDI system.

The decrease in the resistance for both upper and lower parts with time in Fig. 8 can be explained by the electro-regeneration effect. Fig. 9 shows the ion exchange resin, in its hydrogen and hydroxyl ion forms, has a higher electrical conductivity than the same resin in its sodium and chloride forms. This finding indicates that the cell resistance during CEDI operation should decrease as the ionic form

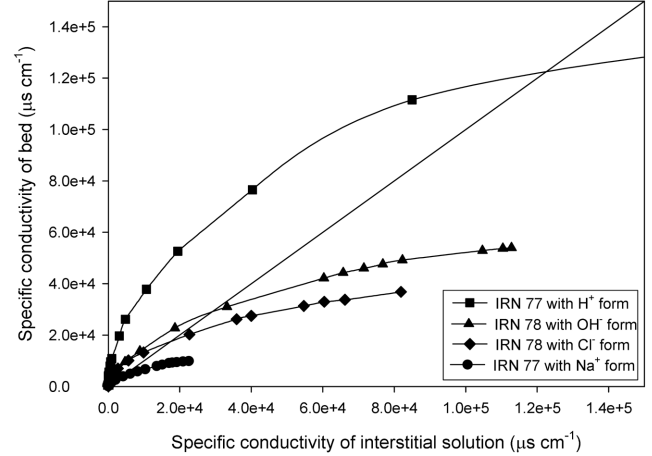


Fig. 9. Electrical conductivity of IRN 77 and IRN 78 with various ionic form.

of the ion exchange resin turns to its hydrogen and hydroxyl forms. Moreover, the regeneration portion with the stack height can be estimated with cell voltage change from Fig. 8. If we assume that the cell potential is caused by ion exchange resins, membranes, and interstitial solution, and water splitting on bipolar interface, cell potential can be expressed with Eq. (5).

$$V_{cell} = I_{stack}(R_{solution} + R_{resins} + R_{membranes}) + \phi_{water\ splitting} \quad (5)$$

If we neglect the membrane resistance compared to solution and resins due to thin thickness, cell potential change with time can be expressed with the following Eq. (6).

$$\Delta V_{cell} = I_{stack}(\Delta R_{solution} + \Delta R_{resins}) + \Delta \phi_{water\ splitting} \quad (6)$$

where,  $\Delta V_{cell}$  : cell potential change with CEDI operation

$I_{stack}$  : stack current

$\Delta R_{solution}$  : resistance change of interstitial solution

$\Delta R_{resins}$  : resistance change of ion exchange resins

$\Delta \phi_{water\ splitting}$  : potential change to cause water splitting

Further,  $\Delta \phi_{water\ splitting}$  and  $\Delta R_{solution}$  should be close to zero if the amount of water splitting is constant and the resistance of interstitial solution does not vary during operation (7) [Song et al., 2004].

$$\Delta V_{cell} = I_{stack} \Delta R_{resins} \quad (7)$$

From Eq. (7), the regenerated fraction of the ion exchange resin can be obtained from the voltage change shown in Fig. 8. Fig. 9 shows that mixed bed resistance (CIX : AIX=2 : 3) with hydrogen and hydroxyl ions showed 5.68 times lower than that composed of sodium and chloride ions. The regenerated fraction was calculated with the resistance change of ion exchange resins from Eqs. (7) and (8).

$$R_{Na^+, Cl^-} - \Delta R_{resins} = x R_{H^+, OH^-} + (1-x) R_{Na^+, Cl^-} \quad (8)$$

where,  $R_{Na^+, Cl^-}$  : resistance of mixed resin with sodium and chloride ion form

$R_{H^+, OH^-}$  : resistance of mixed resin with hydrogen and hydroxyl ion form

x : regenerated fraction of ion exchange resins

From the above equations, regenerated fraction of ion exchange

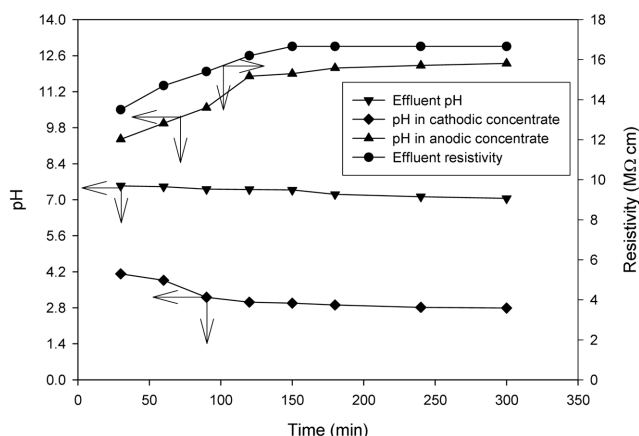


Fig. 10. pH change and effluent resistivity in CEDI system.

resins in the upper part and bottom part were found to be 27.6% and 12.8% during the CEDI operation, respectively. This result shows that the upper part had a higher regenerated fraction than the bottom part. It also implies that electroregeneration mechanism predominantly existed in the upper part.

Fig. 8 also shows the power consumption during a CEDI operation. From the results, the power consumption decreased a little and then was fairly constant for the following operating period, indicating equilibrium between the electroregeneration of the ion exchange resin and ion removal. Fig. 10 shows the profiles of the pH in effluent solution, concentrate 1 (cathodic concentrate), and concentrate 2 (anodic concentrate). It is apparent that high purity water, *i.e.*, 16.7 M $\Omega$ ·cm, was produced and that the effluent pH approached to 7.0 even though slightly alkaline pH was observed initially. Kataoka et al. studied the pH changes while producing high purity water using mixed ion exchange resins [Kataoka et al., 1994]. They also observed that the solution produced was alkaline during the initial operating periods when the feed concentration was less than 100 ppm, even though both the cation and anion exchange resins were mixed in an equal proportion. Moreover, the pH in the cathodic concentrate decreased while that of the anodic concentrate increased. The reason for these changes is the occurrence of water splitting at the bipolar interface formed at the interface between the oppositely charged materials, as shown in Fig. 2.

Table 4. Guidelines for makeup water in a nuclear power plant for selected species

Parameter	Korea nuclear units 3&4	Korea nuclear units 7&8
PH	>6.0	>6.0
	<8.0	<8.0
Resistivity (M $\Omega$ ·cm)	>5	>10
Sodium, ppb	<3	<10
Magnesium, ppb	<40	<20
Calcium, ppb	<40	<20
Chloride, ppb	<5	<5
Sulfate, ppb	<5	-
Silica, ppb	<10	<100

### 3-2. Production of High Purity Water with the CEDI System

High purity water was produced by the CEDI system. Table 3 lists the characteristics of the CEDI effluent, showing that high purity water was produced from the system. The concentration of every species tested in the effluent solution was either very low or not detected and the resistivity of the produced water was 16.7 M $\Omega$ ·cm. The TOC values from Table 3 show that the use of RO system prior to CEDI operation is required for the removal of organic matter. Also, the water quality based on the selected species satisfies the requirements needed for the makeup water in a nuclear power plant, as listed in Table 4. These results demonstrate that the use of the CEDI system after RO to produce high purity water is very feasible.

## CONCLUSIONS

The production of high purity water was carried out using the RO-CEDI hybrid process. The CEDI system showed good performance in producing high purity water, showing a resistivity greater than 15 M $\Omega$ ·cm. A study of the CEDI mechanism verified that the stack consisted of two distinctive regimes, *i.e.*, the enhanced transfer and electro-regeneration regions. The performance of the CEDI operation under the optimized operating conditions showed an ion removal rate of greater than 99%.

## ACKNOWLEDGMENTS

The authors gratefully acknowledge the Basic Atomic Energy Research Institute (BAERI) program at the Korea Institute of Science and Technology Evaluation and Planning (KISTEP) for the financial support to carry out this work.

## REFERENCES

- Ganzi, G. C., Egozy, Y. and Giuffrida, A. J., "High Purity Water by Electrodeionization Performance of the Ionpure Continuous Deionization System," *Ultrapure Water*, April, 43 (1987).
- Ganzi, G. C., Wood, J. H. and Griffin, C. S., "Water Purification and Recycling using the CDI Process," *Env. Progress*, **11**(1), 49 (1992).
- Helfferich, F., *Ion Exchange*, McGraw-Hill, New York, 422 (1962).
- Kataoka, T., Muto, A. and Nishiki, T., "Theoretical Analysis of Mass Transfer of Deionization by Cation and Anion Exchange Resins a Batchwise Contact," *J. Chem. Eng. Japan*, **27**(3), 375 (1994).
- Noh, B. I., Yoon, T. K. and Moon, B. H., "The Mixed Bed Ion Exchange Performances at Ultralow Concentrations," *Korean J. Chem. Eng.*, **13**, 150 (1996).
- Song, J. H., Yeon, K. H. and Moon, S. H., "Transport Characteristics of Co<sup>2+</sup> through an Ion Exchange Textile in a Continuous Electrodeionization (CEDI) System under Electro-regeneration," *Sep. Sci. and Tech.*, **39**, 3609 (2004).
- Spiegel, E. F., Thompson, P. M., Helden, D. J., Doan, H. V., Gaspar, D. J. and Zanapalidou, H., "Investigation of an Electrodeionization System for the Removal of Low Concentrations of Ammonium Ions," *Desalination*, **123**, 85 (1999).
- Spiegler, K. S., *Principles of Desalination*, Academic press, New York, 441 (1966).
- Thate, S., Specogna, N. and Eigenberger, G., "A Comparison of Differ-

- ent EDI Concepts used for the Production of High-purity Water,' *Ultrapure Water*, **OCTOBER**, 42 (1999).
- Walters, W. R., Weiser, D. W. and Marek, L. J., "Concentration of Radioactive Aqueous Wastes," *Ind. and Eng. Chem.*, **47**(1), 61 (1955).
- Yeon, K. H., "Preparation and Characterization of Ion-conducting Spacer in Continuous Electrodeionization and Their Applications in a Nuclear Power Plant," Ph.D Dissertation, Kwangju Institute of Science and Technology, South Korea (2003a).
- Yeon, K. H., Seong, J. H., Rengaraj, S. and Moon, S. H., "Electrochemical Characterization of Ion-exchange Resin Beds and Removal of Cobalt by Electrodeionization," *Sep. Sci. and Tech.*, **38**(2), 443 (2003b).
- Yeon, K. H., Song, J. H. and Moon, S. H., "A Study on Stack Configuration of Continuous Electrodeionization for Removal of Heavy Metal Ions from the Primary Coolant of a Nuclear Power Plant," *Water Research*, **38**, 1911 (2004a).
- Yeon, K. H., Song, J. H. and Moon, S. H., "Preparation and Characterization of Immobilized Ion Exchange Polyurethanes (IEPU) and Their Applications for Continuous Electrodeionization (CEDI)," *Korean J. Chem. Eng.*, **21**, 867 (2004b).